Electronic Supplementary Material (ESI) for Journal of Materials Chemistry B.

Magnetic Proline based Ionic Liquid Surfactant as Nano-carrier for Hydrophobic Drug Delivery

Akshay Kulshrestha,[ab] Praveen Singh Gehlot,[c] Arvind Kumar[ab]*

[a]CSIR-Central Salt and Marine Chemicals Research Institute, Council of Scientific and Industrial Research, G. B. Marg, Bhavnagar, 364002, Gujarat India

[b]Academy of Scientific and Innovative Research (AcSIR), Ghaziabad-201002, India.

[c] Department of chemistry, Government Science College Pardi, Valsad-39612, Gujarat, India

Contents:

1. Structural scheme of synthesized [ProC$_{10}$] [FeCl$_3$Br].

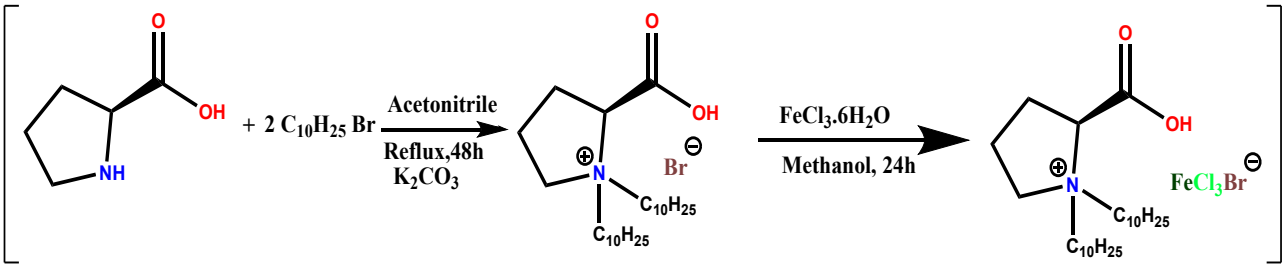

Figure S1. Synthetic procedure of [ProC$_{10}$][FeCl$_3$Br] .

2. ^{1}H NMR of the synthesis of [ProC$_{10}$] [Br]

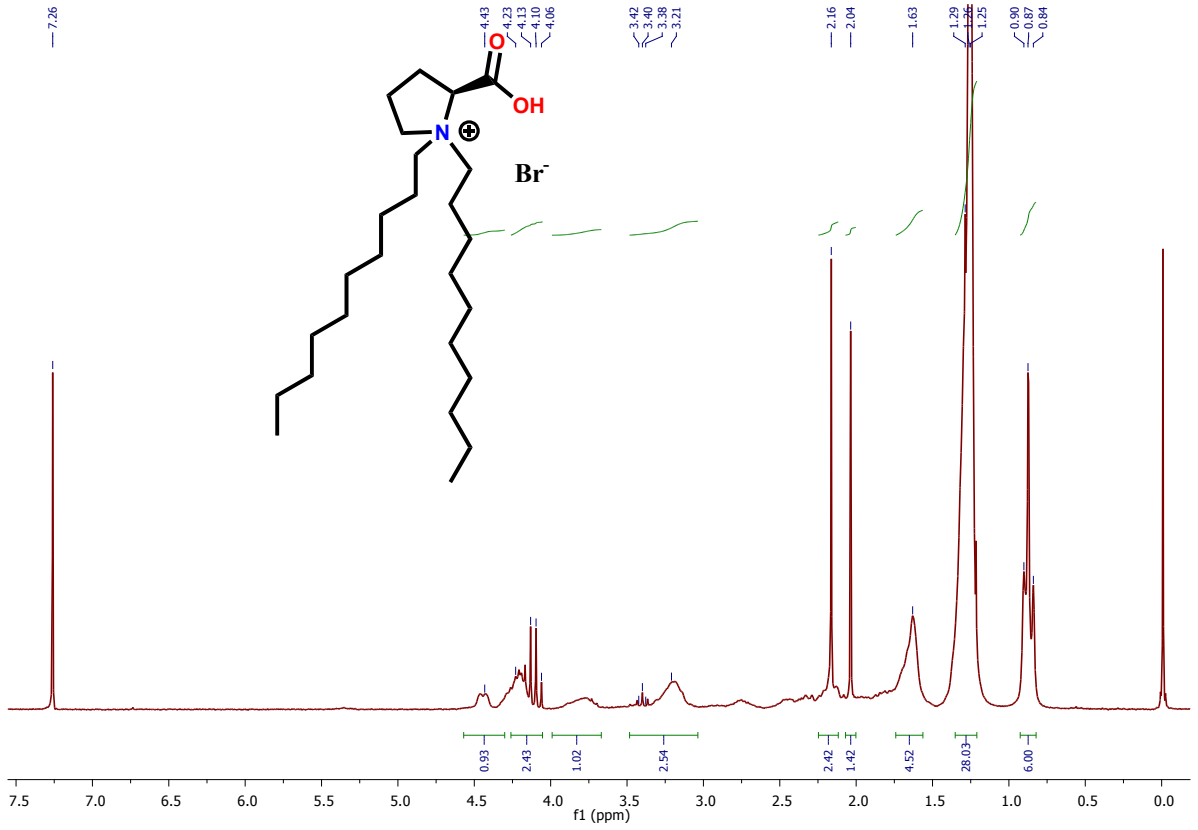

Figure S2. ^{1}H NMR of the synthesis of [ProC$_{10}$] [Br].

^{1}H NMR chemical shift values of [ProC$_{10}$][Br]: $CDCl_3$, 500MH$_z$: δ_H (ppm) 4.3(t, 1H), 4.00(t,2H,NCH2) 3.7 (s,1H,NCH_2),3.21-3.4(m, 3H), 2.16(m, 2H, CH_2), 2.04(m, 2H,CH_2), 1.63 (m,4H,CH_2), 1.25-1.29(m, 28H,CH_2), 0.84-0.90(t,6H,CH_3).

3. Raman spectra and EPR spectra of $[ProC_{10}][FeCl_3Br]$ [1,2]:

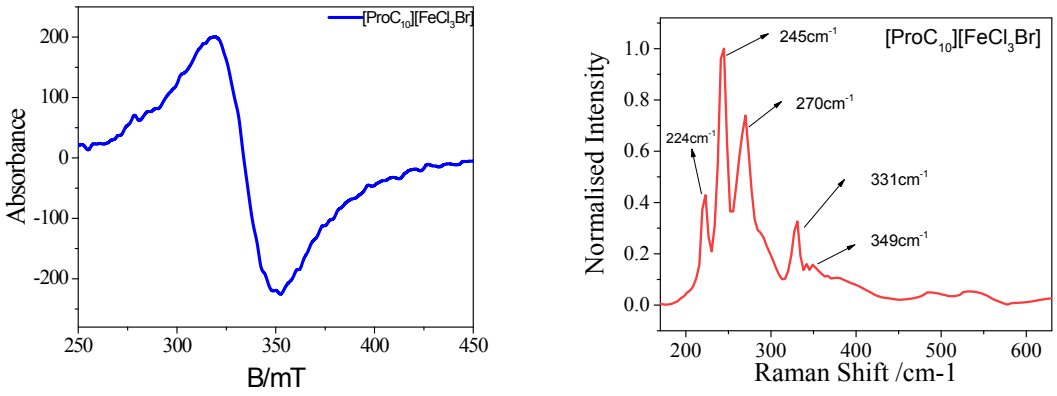

Figure S3. EPR spectra and Raman spectra of $[ProC_{10}][FeCl_3Br]$ respectively.

4. VSM graph of $[ProC_{10}][FeCl_3Br]$

The field dependence magnetic susceptibility has been carried out for $[ProC_{10}][FeCl_3Br]$ at room temperature for a magnetic field range -1.2T to 1.2T. However, there is no opening of hysteresis loop in both the cases. Moreover, there is no saturation upto 1.2T indicating that there are strong magnetic interactions among the metal centres**.**

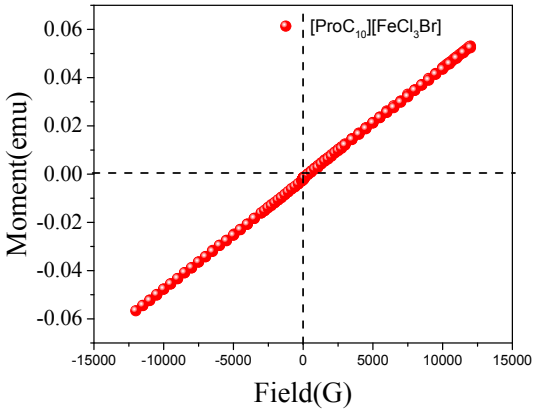

Figure S4. Represents the magnetic moment vs field graph of $[ProC_{10}][FeCl_3Br]$.

5. DSC thermogram of [ProC$_{10}$][FeCl$_3$Br] and various values obtained from TGA and DTG.

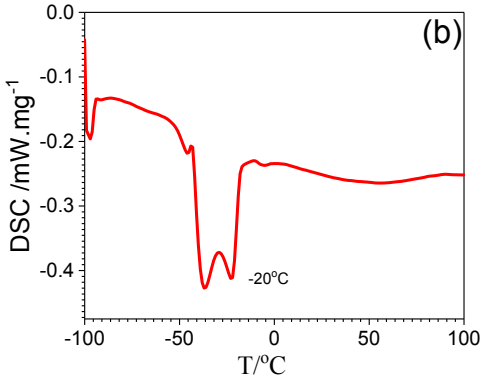

Figure S5 DSC of [ProC$_{10}$][FeCl$_3$Br]

Table S1: T_d, T_{start} and T_{onset} of [Pro C$_{10}$][FeCl$_3$Br] and [Pro C$_{10}$][Br].

MSAILs	**T_{start}(^{o}C)**	**T_d (^{o}C)**	**T_{onset}(^{o}C)**
[Pro C$_{10}$][Br]	148	247	170
[Pro C$_{10}$][FeCl$_3$Br]	220	244	240

6. TEM images of [ProC$_{10}$][Br] .

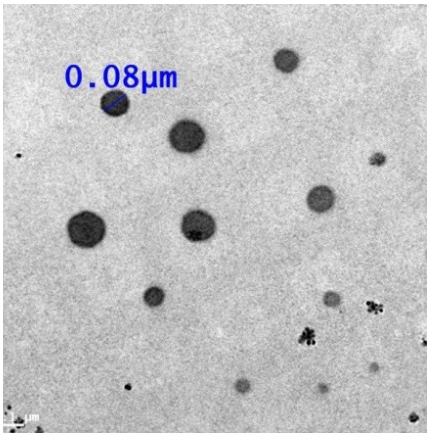

Figure S6.TEM images of [ProC$_{10}$][Br]

7. Autocorrelation Function of MPSAILs

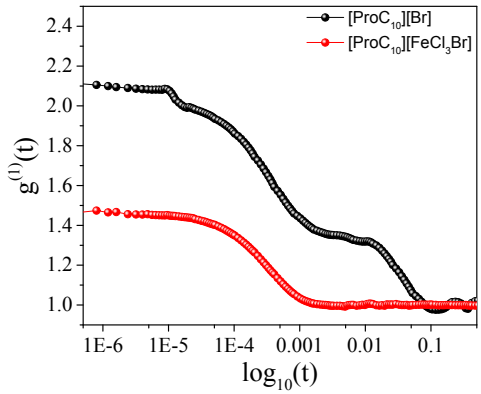

Figure S7 Autocorrelation Function of [ProC$_{10}$][Br] and [ProC$_{10}$][FeCl$_3$Br].

Annexure I

The Surface parameter equation are as follow:[3]

1. The Adsorption efficiency(pC_{20}) and Effectiveness of Surface tension reduction(Π_{CMC}) of surfactant at air-water interface is estimated by using the relation (1)[1,2]

$$pC_{20} = -\log C_{20}, \qquad \pi_{CMC} = \gamma_{H_2O} - \gamma_{CAC} \quad \text{.....(1)}$$

where, C_{20} is the concentration reduce by 20mNm-1 from the surface tension of the solvent (water)[1], γ_{H_2O} stands for the surface tension of the pure water and γ_{CMC} stands for the surface tension of the solvent medium at CMC.

2. The amount of surfactants adsorbed at the interface is estimated from relative surface excess concentration (Γ_{max}).The values Γ_{max} of at the CMC have been calculated using Gibbs adsorption Eq. 2.

$$\Gamma_{max} = -\frac{1}{nRT}\frac{\partial\gamma}{\partial \ln C} \quad \text{.....(2)}$$

where "$\partial\gamma/\partial \ln C$" is the slope of $\gamma - \ln C$ plot in the pre *CMC* region and n is Gibbs adsorption coefficient.

3. Minimum area occupied by monomers at the interface was calculated using equation 4.

$$A_{\min} = \frac{10^{16}}{\Gamma_{\max} . N_A} \quad \text{.....(3)}$$

where N_A is Avogadro number and the Unit of A_{min} is Å^2.

Annexure-II

Table S2: Various mathematical models and their equations:[4]

Mathematical Model	Equation
Zero Order	$C_o - C_t = K_o t$
First Order	$\ln C = \ln C_o - K_1 t$
Higuchi model	$Q = A\sqrt{D(2Co - Cs)Cst}$
Hixson–Crowell model	$C_0^{1/3} - C_t^{1/3} = K_{HC} t$
Korsmeyer- Peppas model	$M_t/M_\infty = K_{kp}\, t^n$

where C_o = intial concentration of the drug at time, t = 0, C_t = amount of drug released at time t, K_o = zero order constant, K_1 = first order rate constant, C = percent of drug remaining at time t,Q=Cumulative amount of drug released at time per unit area, C_S is the drug solubility in the matrix and D is the diffusion coefficient of the drug molecule in the matrix, C_S =drug solubility in the matrix and D =diffusion coefficient of the drug molecule in the matrix.Mt = amount of drug released in time t, M∞ = amount of drug released after time ∞, n = diffusional exponent or drug release exponent, and K_{kp} = Korsmeyer release rate constant.

Table S3. A comparison of loading efficiency of ciprofloxacin drug in various surfactants or polymeric colloidal systems.

S.No	Surfactant/ polymer	Drug Carrier	Loading efficiency (%)	Author	Year
1.	Present work $[ProC_{10}][FeCl_3Br]$	vesicles	84.2%	-	-
2.	Ciprofloxacin-HCl-Chitosan/Tween/Tri polyphosphate	Micelle nanocomposite	45-56%	Manea et al.[52]	2019
3.	Block copolymers, poly(ε-caprolactone)-block-poly(lysine-stat-phenylalanine bioflim	vesicles	13-31%	Xi et al.[55]	2019
4.	Pluronics (Pluronic F108 and Pluronic L81)	Micelles	N.R.	Senthilkumar et al.[56]	2019
5.	Long chain non-ionic surfactant N-(4-sulfamoylphenyl)dodecanamide	Vesicles	68-82%	Ali et al.[57]	2019
6.	(N-butyl acetate/polysorbate 80/ethanol/water)	Microemulsion	3.6%	Saleem et al.[58]	2018
7.	Effect of NaCl on interaction between SDS and HTEAB	micelles	N.R	Banipal et al.[59]	2018
8.	Poly(ethylene oxide) (PEO), a surfactant Pluronic F-127	Nanofibre	51%	Kyzioł et al.[60]	2017
9.	Surfactant method for core–shell mesoporous silica based layered double hydroxide	disc-like morphology	37%	Barnabas et al.[61]	2017
10.	Diacyl glycerol-arginine surfactants	vesicle	8-13%	Tavano et al.[62]	2014

Table S4: Kinetics study of release of guest molecule by various mathematical models.

Guest Molecule	Release condition	*Zero Order		*First order		*Higuchi Model		*KorsMeyar Peppas		*Hixon Crowell	
		R^2	Slope	R^2	Slope	R^2	Slope	R^2	Slope	R^2	Slope
Pyrene	pH 7	0.78	0.17	0.85	0.002	0.87	3.3	0.95	0.44	0.83	0.005
Ciprofloxacin	pH 7	0.92	1.19	0.99	0.015	0.97	11	0.99	0.69	0.97	0.037

REFERENCE

1. Döbbelin, M.; Jovanovski, V.; Llarena, I.; Marfil, L. J. C.; Cabañero, G.; Rodriguez, J.; Mecerreyes, D. Synthesis of paramagnetic polymers using ionic liquid chemistry. *Polymer Chemistry* **2011**, *2*(6), 1275 DOI: 10.1039/c1py00044f.
2. Shongwe, M. S.; Al-Rahbi, S. H.; Al-Azani, M. A.; Al-Muharbi, A. A.; Al-Mjeni, F.; Matoga, D.; Gismelseed, A.; Al-Omari, I. A.; Yousif, A.; Adams, H.; et al. Coordination versatility of tridentate pyridyl aroylhydrazones towards iron: tracking down the elusive aroylhydrazono-based ferric spin-crossover molecular materials. *Dalton Transactions* **2012**, *41*(8), 2500 DOI: 10.1039/c1dt11407g.
3. Rosen, M. J.; Mathias, J. H.; Davenport, L. Aberrant Aggregation Behavior in Cationic Gemini Surfactants Investigated by Surface Tension, Interfacial Tension, and Fluorescence Methods. *Langmuir* **1999**, *15*(21), 7340–7346 DOI: 10.1021/la9904096.
4. Baishya, H. Application of Mathematical Models in Drug Release Kinetics of Carbidopa and Levodopa ER Tablets. *Journal of Developing Drugs* **2017**, *06*(02) DOI: 10.4172/2329-6631.1000171.